

# RESISTIVITY IMAGING AND IMAGE ANALYSIS FOR ESTIMATING WATER AND SOLUTE TRANSPORT ACROSS THE CAPILLARY FRINGE IN LABORATORY EXPERIMENTS

Resistivitet mätningar och bildanalys för att uppskatta vatten och partikeltransport genom den kapillära zonen i laboratorieexperiment

PONTUS POJMARK<sup>1</sup>, BENEDICT RUMPF<sup>2</sup>, TORLEIF DAHLIN<sup>2</sup>,  
MAGNUS PERSSON<sup>1</sup>, and THOMAS GÜNTHER<sup>3</sup>

<sup>1</sup> Department of Water Resources Engineering, Lund University, 211 00 Lund, Sweden

<sup>2</sup> Department of Engineering Geology, Lund University, 211 00 Lund, Sweden

<sup>3</sup> Leibniz-Institute for Applied Geophysics (LIAG), Stilleweg 2, 30655 Hannover, Germany



## Abstract

This study contains a series of laboratory experiments designed to describe the lateral movement and spatial variability of an infiltrated dye tracer across the capillary fringe of homogenous sand in an aquarium. A combination of image analysis and geoelectrical monitoring was used to track the flow paths of the dye with different hydraulic gradients and infiltration rates. Photographs were taken for image analysis to visualize the flow paths. An ABEM Terrameter LS was used to measure the resistivity data during the experiments with a combination of multiple-gradient array and cross-hole-dipole-dipole array. BERT (Boundless Electrical Resistivity Tomography) was applied to obtain three dimensional models of the resistivity distribution. The results were compared and evaluated in respect to the image analysis. The inverted models gave a clear impression of the dye tracer distribution and movement within the aquarium. All experiments revealed a strong horizontal movement across the capillary fringe. The flow characteristics of the capillary fringe turned out to be more similar to the characteristics of the saturated zone, than to the characteristics of the unsaturated zone. If the results of this laboratory study can be verified under field conditions, it clearly shows that taking measurements and samples only in the saturated zone at contaminated sites can significantly underestimate the actual extent of the contamination plume.

*Key words* – capillary fringe, lateral movement, dye tracer, image analysis, geoelectrical imaging, resistivity, BERT

## Sammanfattning

Denna undersökning innehåller en serie laboratorieexperiment utförda för att beskriva den laterala rörelsen av ett infiltrerat spårämne genom den kapillära zonen för en homogen sand i ett akvarium. En kombination av bildanalys samt geoelektrisk mätning användes för att spåra olika flödesvägar som spårvätskan tog vid olika hydrauliska gradienter och infiltrationshastigheter. Fotografier användes i bildanalysen för att visualisera spårämnets väg på en sida av akvariet. En ABEM Terrameter LS användes för att mäta resistivitetdata under experimenten med en kombination av multiple-gradient protokoll och cross-hole-dipole-dipole protokoll. BERT (Boundless Electrical Resistivity Tomography) användes för att erhålla tredimensionella modeller av resistivitet distributionen. Resultaten utvärderades och jämfördes med hänsyn till bildanalysen. De inverterade modellerna gav en tydlig bild över spårämnets distribution och flödesväg i akvariet. Alla experiment visade en kraftig horisontell rörelse i den kapillära zonen. De hydrauliska egenskaperna i den kapillära zonen visade sig vara mer lika egenskaperna i den mättade zonen än för den omättade zonen. Om resultaten i studien kan verifieras i fältförsök visar det att om man enbart mäter och tar prover i den mättade zonen på en förorenad plats är det risk för att man underskattar den faktiska volymen av föroreningen kraftigt.

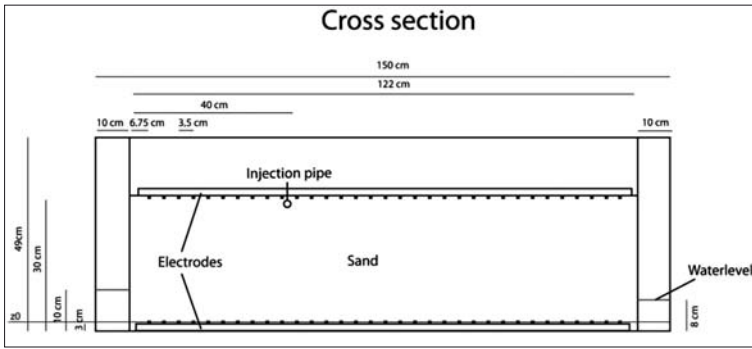


Figure 1. Cross section of the aquarium layout.

## Introduction

The rapid population growth combined with industrialization and urbanization results in an increasing demand for water and threatens the livelihoods of many people. Therefore, the maintenance and protection of groundwater, the largest freshwater resource in many areas, becomes one of the biggest challenges of our times. To assure a secure water supply for drinking, industry and agriculture it is essential to avoid groundwater contaminations and therefore to understand the subsurface water movement.

The hydrological cycle and its steps between precipitation and groundwater runoff are well known and were described e.g. by Fetter (2001), or Press and Siever (2003). The saturated as well as the unsaturated zone have been subject of many water movement surveys over the last decades (see e.g. Wellings and Bell, 1982; McMahon et al., 2001; Mali et al., 2006; Mikulec and Orfanus, 2005). However, the influence and complexity of the region of transition between these zones, the capillary fringe, has been more or less neglected in water movement investigations. Although a lateral movement of water within the capillary fringe was recognized by Luthin and Day already in 1955, the role of the capillary

fringe in lateral transport of water and pollutants has not completely been explained in groundwater literature. Recent studies showed that this role might be more significant than expected.

The aim of this study was to analyse the lateral movement of water and solutes in the capillary fringe, regarding the impacts of the unsaturated infiltration rate and the hydraulic gradient of the groundwater table, by using a combination of image analysis and geoelectrical monitoring.

## Materials and methods

The model used in this study involved a 150 cm long, 49 cm high and 48 cm deep glass aquarium. It consisted of 3 basins which were separated by perforated walls covered with a permeable geotextile. The main basin had a width of 122 cm and was situated between two smaller basins, each with a width of 10 cm. The main basin was filled up to a height of 32 cm with homogeneous sand. The sand had a grain size of 0.3–0.7 mm and allowed a capillary fringe of 13 cm above the saturated zone. The thickness of the saturated zone could be regulated by changing the water levels in the two smaller basins on

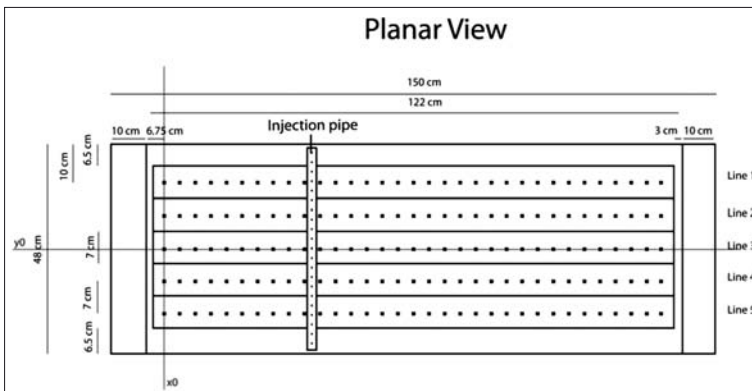


Figure 2. Planar view of the aquarium layout.

Figure 3. Image of experiment 2, 3 hours after starting the dye infiltration.

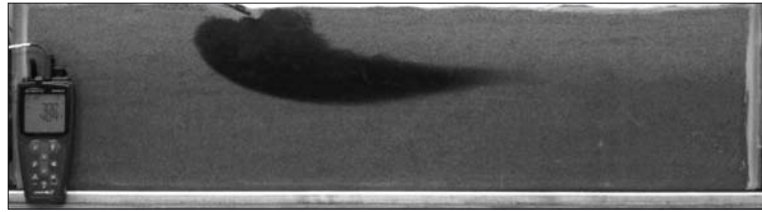
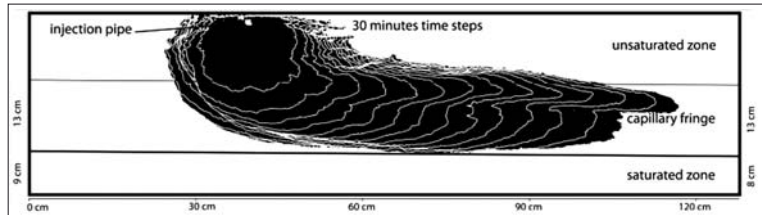


Figure 4. Combined template image, illustrating the dye tracer movement in 30 minutes time steps in experiment 3.



both sides of the aquarium. A pump system was installed to circulate water through the aquarium and regulate the gradient across the basin. The maximum water level varied between 9 and 12 cm. Therefore it was possible to establish a three-layer regime within the aquarium, including the saturated zone, the capillary fringe and an unsaturated zone of approximately 8 – 10 cm on top.

Infiltration of the dye tracer Brilliant Blue FCF was regulated by a pump and injected through a pipe system on the sand surface. To keep the same water levels, even after the injection of the dye tracer, another pump was connected to a level gauge in the right basin, which extracted the same amount of water that was injected in form of the tracer. The cross sections of the aquarium can be seen in Figures 1 and 2.

Photographs taken at a regular time interval of 3 minutes were used for the image analysis to visualize the flow paths through the front side of the aquarium (see Figure 3). Every tenth picture, which corresponds to a time interval of 30 minutes, was modified with Adobe Photoshop CS™ and Adobe Illustrator CS™ to create a black and white template image. These modified template images were then combined to present the tracer distribution throughout the experiments in relation to the soil water regime within the aquarium (see Figure 4). The indication of the 30 minutes time steps can be used to measure the average propagation velocity of the dye tracer by correlating the travelled distance with time (30 minutes).

An ABEM Terrameter LS was connected to a customised electrode system to measure the resistivity data during the experiments. Ten lines of electrodes were used, five in the bottom and five on top of the sand, containing a total of 320 electrodes (see Figures 1 and 2). The electrode spacing was 3.5 cm. A combination of mul-

tiple-gradient array and cross-hole-dipole-dipole array was used for taking measurements along and between the electrodes on top of and in the bottom of the sand.

The Boundless Electrical Resistivity Tomography (BERT) software, which is described in Günther et al., 2006, was used to obtain a three dimensional model of the resistivity distribution within the aquarium. Based on the coordinate axes  $x_0$ ,  $y_0$  and  $z_0$ , seen in Figures 1 and 2, dimensions and boundary conditions of the aquarium were implemented and different inversion parameters were adjusted to improve the model quality. A MATLAB® script created a ratio between the resistivity values taken during the experiments and a background measurement which was taken before each experiment. ParaView was used to visualise the gained model with a 'grey to white' colour scheme. Grey colour represents ratio values smaller than 1, which corresponds to a decrease of resistivity. Areas with no change in resistivity (ratio = 1) were presented white. An example of these three dimensional plots can be seen in Figure 5.

The results of the geoelectrical monitoring were evaluated in respect to the correlation of the results of the image analysis by comparing the side views of the 3D ratio plots with the corresponding shape of the dye distribution from the image analysis (Figures 8 and 9).

## Results and Discussion

Five experiments were conducted to investigate the lateral movement of the dye tracer within the capillary fringe of sand. The different experimental setups, including variations in the hydraulic gradient and the unsaturated infiltration rate can be seen in table 1.

All experiments revealed a strong horizontal move-

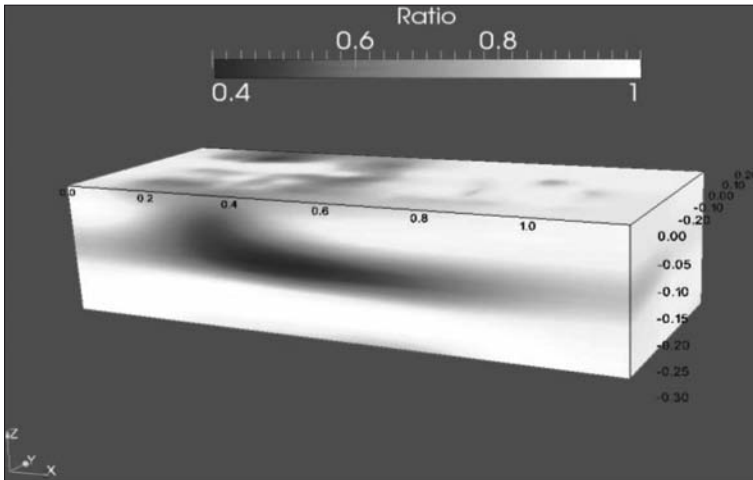


Figure 5. 3D ratio plot of the difference in resistivity caused by the infiltration of the dye tracer during experiment 4 after 4 hours.

ment across the capillary fringe. The results of the image analysis (Figure 4) show that the infiltrated dye tracer percolated vertically through the unsaturated zone, but moved horizontally as soon as it reached the capillary fringe, without intersecting the saturated zone.

Table 2 contains a comparison between the measured and the calculated velocity for each experiment. The total volume of fluids, including the infiltrated dye tracer and the circulating water, was taken into account for the calculations. It was assumed that the movement in the capillary fringe is equal to the movement in the saturated zone, since the observation indicated a high horizontal flow within the capillary fringe. The comparison shows a big discrepancy and demonstrates that the velocity in the capillary fringe is lower than in the saturated zone. In fact, the values prove that the velocity within the capillary fringe is dependent on the penetration depth of the dye and is decreasing with distance to the saturated zone. The dye in experiment 3 reached deepest down and moved with a velocity of approximately 60 % of the saturated flow velocity. In experiment 5 the dye barely infiltrated the capillary fringe and travelled with a velocity of only 30 % of the saturated flow velocity.

The influences of the different experimental setups on the flow patterns can be described, while looking at the comparisons in Figures 6 and 7. Figure 6 shows the distribution of the dye tracer in experiments 1, 2 and 3 after four hours and proves that the velocity in the capillary fringe is highly dependent on the hydraulic gradient of the saturated zone. The dye in experiment 2 travelled much further than in the other two experiments after the same time. The hydraulic gradient of the saturated zone also affects the vertical movement within the capillary fringe. The penetration depth increases as the hydraulic gradient decreases. However, the template image of experiment 3 (Figure 4) proves that even with a small gradient the dye does not intersect the water table in the aquarium.

Figure 7 illustrates the influence of the injection rate of the dye on the transport across the capillary fringe. The comparison between experiments 2 and 5 proves that the injection rate mainly influences the penetration depth of the dye. While the dye penetrates half way through the capillary fringe in experiment 2, it almost seems to float above the capillary fringe in experiment 5. The velocity seems to be independent of the injection rate.

Table 1. Experimental setups.

	Infiltration rate [l/h]	Circulating flow [l/h]	Hydraulic gradient [cm]	Corresponding angle [°]	Duration [h]
Experiment 1	2	4	2	0.93	4
Experiment 2	2	8	4	1.88	5
Experiment 3	2	2	1	0.47	7
Experiment 4	0.8	4	2	0.93	6.5
Experiment 5	0.8	8	4	1.88	6

Table 2. Comparison of the measured and calculated velocity.

	Measured velocity, $v_m$ [cm/h]	Calculated velocity, $v_c$ [cm/h]	$v_m/v_c$ [%]
Experiment 1	6.32	13.51	46.8
Experiment 2	9.47	22.05	42.9
Experiment 3	5.53	8.79	62.9
Experiment 4	3.95	9.1	43.4
Experiment 5	8.68	28.5	30.5

While looking at the comparisons between the results of the image analysis and the models created with BERT, shown in Figures 8 and 9, it should be mentioned that finding optimum parameters of the BERT-software turned out to be difficult. The long processing time BERT needed to test each configuration made it necessary to use the most acceptable solution achieved, and not the optimal solution. However, the comparisons

mentioned above prove that the BERT-configuration used in this thesis was able to produce reliable results. The overall similarity of the shapes of the dye distributions can be seen in all experiments. In general, the plumes of the model are bigger than the plumes of the image analyses and seem to have smoother borders. But it must be considered that the borders of the image analysis only seem to be that distinguished because of

Figure 6. Comparison of the dye tracer distribution for different hydraulic gradients after four hours. The indicated water level and the level of the capillary fringe correspond to experiment 1 and are not valid for experiment 2 and 3.

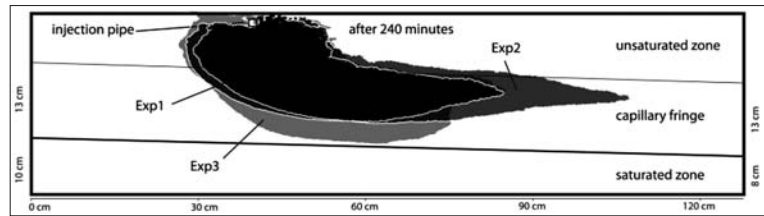


Figure 7. Comparison of the dye tracer distribution for different injection rates after four hours. Exp2: 2.0 l/h, Exp5: 0.8 l/h.

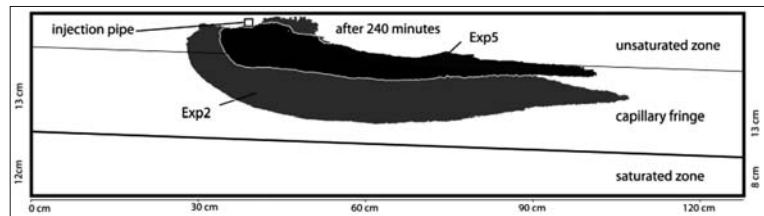


Figure 8. Comparison between the result of the image analysis and the 3D model produced with BERT of experiment 1, after ca. 3 hours. Grey colour indicates a decrease in the resistivity compared to the background measurement.

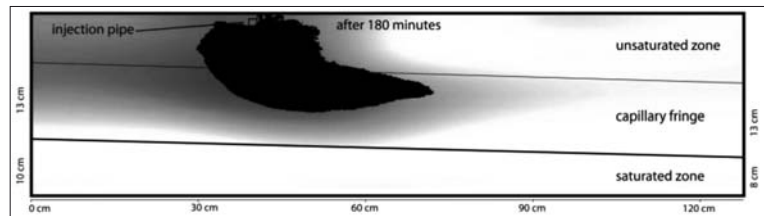
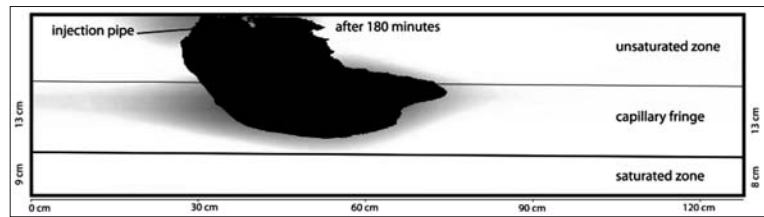


Figure 9. Comparison between the result of the image analysis and the 3D model produced with BERT of experiment 3, after ca. 3 hours. Grey colour indicates a decrease in the resistivity compared to the background measurement.



the schematic presentation method. The original photographs show a decreasing concentration of dye in the outer parts of the plume. The difference in the sizes of the plumes can be explained with the different minimal detection limits of the methods. While the resistivity analysis can measure even smallest changes caused by minimal variations in the concentration of dye, the lowest with human eyes detectable concentration of dye in sand is about 0.1 g/l.

It is interesting to note that in all experiments even if the plume of the modelled dye tracer distribution is bigger than the one seen in the image analysis, the dye never reaches the saturated zone.

## Conclusion

The goal of this study was to analyse the water and solute transport across the capillary fringe using a combination of image and resistivity analysis. The comparison between the image analysis and the side views of the 3D models showed a clear correlation and therefore indicate a high reliability for the inversion. The models gave a clear impression of the dye distribution in the whole aquarium and proved that ERT can be a very useful tool for subsurface investigations.

The comparison of the experiments with different hydraulic gradients and infiltration rates revealed a high horizontal movement across the capillary fringe. In all experiments, the dye tracer moved vertically through the unsaturated zone, but moved laterally within the capillary fringe without intersecting the saturated zone. The velocity of this movement proved to be highly dependent on the hydraulic gradient of the saturated zone. The infiltration depth was influenced by the infiltration rate of the dye tracer.

The flow characteristics of the capillary fringe turned out to be more similar to the characteristics of the saturated zone, than to the characteristics of the unsaturated zone. If the result of this laboratory study can be verified under field conditions, it clearly shows that taking measurements and samples only in the saturated zone at contaminated sites can significantly underestimate the actual extent of the contamination plume.

## References

- Fetter, C.W. (2001) Applied Hydrogeology, Fourth Edition, Prentice-Hall Inc.
- Günther, T., Rücker, C., and Spitzer, K. (2006) 3-D modelling and inversion of dc resistivity data incorporating topography – part II: Inversion. *Geophys. J. Int.*, 166(2):506–517.
- Luthin, J.N., and Day, P.R. (1955) Lateral flow above a sloping water table. *Soil Sci. Soc. Of Am. Proc.* 19: 406–410.
- Mali, N., Urbanc, J., and Leis, A. (2006) Tracing of water movement through the unsaturated zone of a coarse gravel aquifer by means of dye and deuterated water, *Environmental Geology*, Volume 51, Number 8, p. 1401–1412, Springer.
- McMahon, P.B., Dennehy, K.F., Michel, R.L., Sophocleous, M.A., Ellet, K.M., and Hurlbut, D.B. (2001) Water Movement Through Thick Unsaturated Zones Overlying the Central High Plains Aquifer, Southwestern Kansas, 2000–2001, USGS, Water Resources Investigations Report 03-4171.
- Mikulec, V. and Orfanus, T. (2005) Numerical Simulation of Soil Water Movement in Variably Saturated Zone of Heterogeneous Soil Profile during Growing Period of Corn, *Geophysical Research Abstracts*, Vol 7, European Geoscience Union 2005.
- Press, F. and Siever, R. (2003) *Allgemeine Geologie, Einführung in das System Erde*, 3. Auflage, Spektrum.
- Wellings, S.R., and Bell, J.P. (1982) Physical controls of water movement in the unsaturated zone, *Quarterly Journal of Engineering Geology and Hydrogeology*, 15, 235–241.